Journal of ELECTRONIC MATERIALS, Vol. 36, No. 4, 2007
DOI: 10.1007/s11664-007-0099-3

Optimization of High-Quality AlN Epitaxially Grown on (0001) Sapphire by Metal-Organic Vapor-Phase Epitaxy

Y.A. XI,[1] K.X. CHEN,[1] F. MONT,[2] J.K. KIM,[2] E.F. SCHUBERT,[1,2,4] C. WETZEL,[1] W. LIU,[3] X. LI,[3] and J.A. SMART[3]

1.—Future Chips Constellation, Department of Physics, Applied Physics, and Astronomy, Rensselaer Polytechnic Institute, Troy, NY 12180, United States. 2.—Future Chips Constellation, Department of Electrical, Computer, and Systems Engineering, Rensselaer Polytechnic Institute, Troy, NY 12180, United States. 3.—Crystal IS, Inc, Green Island, NY 12183, United States. 4.—e-mail: efschubert@rpi.edu

A systematic study is performed to optimize aluminum nitride (AlN) epilayers grown on (0001) sapphire by metal-organic vapor-phase epitaxy. Specifically, the impact of the AlN nucleation conditions on the crystalline quality and surface morphology of AlN epilayers is studied. Atomic force microscopy (AFM) and x-ray diffraction (XRD) results reveal that the nucleation layer plays a critical role in the growth of subsequent layers. The magnitude of the TMAl flow of AlN nucleation layer is found to have a strong effect on the crystalline quality and surface morphology of the high-temperature (HT) AlN epilayer. A simple Al adatom-diffusion-enhancement model is presented to explain the strong dependence of the crystalline quality and surface morphology on TMAl flow. Furthermore, ammonia flow, nucleation temperature, and growth time of the AlN nucleation layer are found to affect the surface morphology and the crystalline quality as well. A trade-off is found between surface morphology and crystalline quality; that is, we do not obtain the best surface morphology and the highest crystalline quality for the same growth parameters. For optimized AlN nucleation layers and HT AlN epilayers, a clear and continuously linear step-flow pattern with saw-tooth shaped terrace edges is found by AFM on AlN epilayers. Triple-axis x-ray rocking curves show a full-width at half-maximum (FWHM) of 11.5 arcsec and 14.5 arcsec for the (002) and (004) reflection, respectively. KOH etching reveals an etch-pit density (EPD) of 2×10^7 cm^{-2}, as deduced from AFM measurements.

Key words: metal-organic vapor-phase epitaxy, nitrides, AlGaN, light emitting diodes

Aluminum nitride (AlN) has generated much interest due to unique properties such as its very wide and direct bandgap and high thermal conductivity. High-quality AlN epilayers are needed in AlGaN ultraviolet (UV) light-emitting diodes (LEDs), which have great potential for applications such as fluorescence-based biological agent detection, water purification, sterilization, decontamination, non-line-of-sight communications, and thin-film curing.[1] At the same time, deep UV photodetectors need extremely high-quality AlN with low dislocation density for the reduction of the dark current. Many efforts have been made in order to improve the crystalline quality of AlN and to decrease the dislocation density.[2–9] Nevertheless, the current crystalline quality of epitaxial AlN must be improved, particularly for UV LEDs and photodetectors.

In this article, we report on the growth of AlN epilayers on (0001) sapphire using the low-temperature (LT) AlN nucleation scheme.[10] The material quality of the AlN epilayers grown on sapphire is determined by atomic force microscopy (AFM) and x-ray diffraction (XRD). A systematic optimi-

(Received July 17, 2006; accepted November 27, 2006; published online May 1, 2007)

zation study of the nucleation layer reveals that the trimethylaluminum (TMAl) flow is a most critical parameter which has a major effect on the surface morphology and crystalline quality. Further study shows that we do not achieve high crystalline quality and good surface morphology simultaneously. After the optimization of nucleation and high-temperature (HT) AlN epitaxial growth, AlN on (0001) sapphire with very high crystalline quality and surface morphology is obtained as assessed by AFM, XRD, etch-pit density (EPD) measurements, and scanning electron microscopy (SEM).

The AlN epilayers are grown using an Aixtron 200/4-RF S low pressure metal-organic vapor-phase epitaxy system with a 5.0-cm single-wafer horizontal-flow geometry and radio-frequency heating. TMAl and NH_3 are used as precursors with H_2 as a carrier gas. Growth is initiated by a LT AlN nucleation layer grown at 50 mbar followed by a 1.0-μm-thick HT AlN layer grown at 25 mbar on (0001) sapphire substrates. The nucleation optimization study involves four series of samples. The first series of samples (samples A and B) is grown with different NH_3 flow. The NH_3 flow/TMAl flow is 1200 sccm/30 sccm and 600 sccm/30 sccm, respectively. The second series (samples B through D) is grown with decreasing TMAl flow of 30 sccm, 20 sccm, and 10 sccm. The third series (samples D through F) uses a growth temperature of 812°C, 840°C, and 850°C. The fourth series (samples E, G, and H) is grown using growth times of 2 min, 1.5 min, and 2.5 min. In all growth runs, the TMAl pressure is 1,000 mbar and the TMAl bubbler temperature is 17°C. Table 1 summarizes the nucleation layer growth conditions of the eight samples.

After the epitaxial growth, the surface morphology and crystalline quality are evaluated by AFM and XRD measurements, respectively. A PANalytical PW3040/60 X'Pert Pro system (PANalytical, Almelo) with triple-axis optics (double-crystal optics with the analyzer crystal) and double-crystal optics is used to measure x-ray rocking curves. The full width at half maximum (FWHM) of the (002) peak of samples A and B is 592 arcsec and 632 arcsec, respectively, measured by double-crystal optics. Many openings are observed on the AlN surfaces through AFM measurements, as shown in Fig. 1. By changing ammonia flow from 1,000 sccm to 600 sccm, no obvious improvement is obtained. Further study is done to decrease TMAl flow for samples B, C, and D. The AFM images of samples B, C, and D are shown in Fig. 2. By decreasing the TMAl flow during the nucleation, the openings start to coalesce on sample C with TMAl of 20 sccm, as shown in Fig. 2. A step-flow terrace is observed on sample D with TMAl of 10 sccm. At the same time, the XRD data reveal that, by decreasing the TMAl flow of the AlN NL, the FWHM of (002) peak of the AlN epilayers decreases by a factor of 13 from the 623 arcsec of sample B to 47 arcsec of sample D. Such tremendous quality improvement comes from the TMAl flow change, which indicates that TMAl flow is a most critical parameter that determines the AlN epilayer crystalline quality.

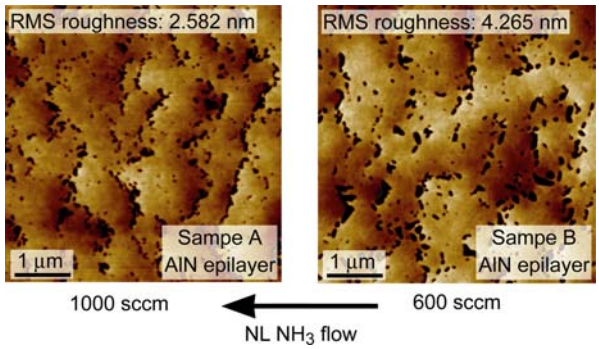

Fig. 1. AFM images of Sample A and B with ammonia flow for AlN NL decreasing from 1000 sccm to 600 sccm.

Based on the evolution of the surface morphology, next, we briefly present a simple Al adatom diffusion-enhancement model to explain the strong dependence of the crystalline quality and the surface morphology on TMAl flow. In the mass-transport limited-growth regime, the growth rate is determined by the TMAl flow. For high TMAl flows, i.e., the sample B case, Al adatoms may not have enough time to fully wet the substrate by diffusion before the next atomic layer is deposited. Therefore, after the HT AlN growth, many openings are

Table I. Nucleation Layer (NL) Growth Conditions of Eight Samples Including NH_3 Flow, TMAl Flow, Growth Temperature, and the Growth Time

Sample	NH_3 Flow (sccm)	TMAl Flow (sccm)	Temperature (°C)	Time (min)
A	1,000	30	812	2
B	600	30	812	2
C	600	20	812	2
D	600	10	812	2
E	600	10	840	2
F	600	10	850	2
G	600	10	840	1.5
H	600	10	840	2.5

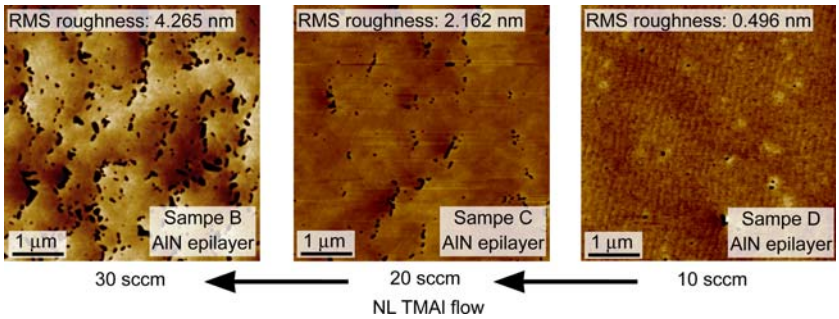

Fig. 2. AFM images of Sample B, C, and D with TMAl flow for AlN NL decreasing from 30 sccm to 10 sccm.

observed on the surface. By lowering the TMAl flow of AlN NL, Al adatoms have more time to fully wet the substrate, which reduces the density of openings on the HT AlN surface. Meanwhile, high temperature and low V/III ratio also result in improving the diffusion of Al adatoms for AlN growth. The inspection of the results of samples A and B reveals that lowering the V/III ratio by decreasing ammonia flow does not strongly improve the crystalline quality, or, according to our model, the diffusion of Al adatoms.

By using a TMAl flow of 10 sccm, different growth temperatures have been employed in order to verify the mechanism of the diffusion improvement. The AFM images of sample D through F are shown in Fig. 3. The FWHMs of the (002) peak of samples D through F are 47 arcsec, 54 arcsec, and 47 arcsec, respectively. From the root-mean-square (RMS) roughness and FWHM results, no clear temperature dependence of the crystalline quality is found. The different trends between the FWHM and surface roughness also indicate that high crystalline quality and good surface morphology are not readily achievable at the same time. Because crystalline quality and surface morphology both play very important roles in epitaxial growth, a balance between them is needed for epitaxial growth on AlN buffer layers.

In order to differentiate the growth rate and NL thickness effect on the surface morphology and the crystalline quality measured by XRD, an NL thickness study is performed. Figure 4 shows 20 μm $\times$ 20 μm size AFM images of samples G, E, and H. The opening density of samples G and H is much higher than that of sample E, which means that 2 min is very good growth time for the AlN NL.

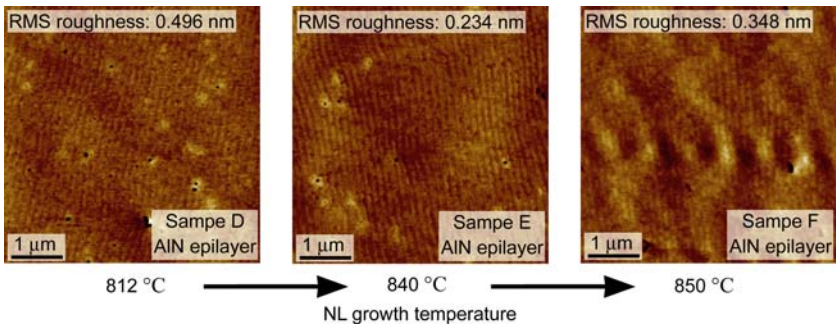

Fig. 3. AFM images of Sample D, E, and F with AlN NL growth temperature increasing from 812°C to 850°C.

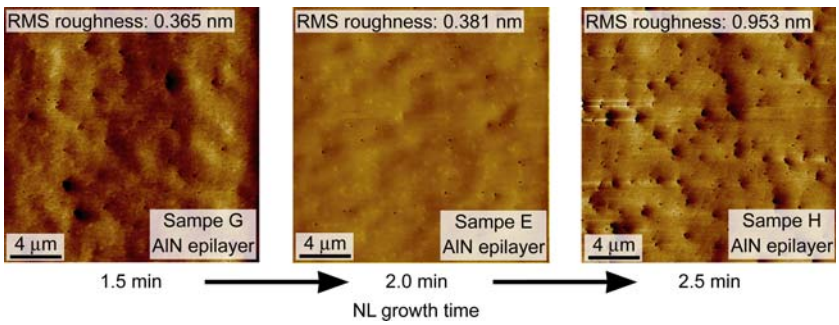

Fig. 4. AFM images of Sample G, E, and H with increasing AlN NL growth time from 1.5 min to 2.5 min.

The FWHMs of the (002) peak of samples G, E, and H are 54 arcsec, 54 arcsec, and 47 arcsec, respectively. Therefore, the AlN NL thickness does not have a strong effect on the crystalline quality but plays an important role in the surface morphology formation.

From our study, we also find that, when the TMAl flow rate is not optimized, the NL growth time affects both the crystalline quality and the surface morphology. However, we could not obtain flat surfaces (RMS < 1 nm for 5 μm × 5 μm image size) and good crystalline quality (FWHM of (002) peak < 0.1 deg). The surface and crystalline quality of the AlN templates with unoptimized TMAl flow are similar to samples A and B. For samples B through D, the TMAl flow rate is changed while using optimized growth time (2 min). Both the surface morphology and crystalline quality are *strongly* affected. For samples G, E, and H in Fig. 4, the NL layer growth time is changed while using optimized TMAl flow (10 sccm). Only the surface morphology is affected. From the above discussion, we believe that the TMAl flow rate plays a more important role than the NL layer thickness.

After the AlN NL optimization, a systematic study is also done to optimize HT AlN growth. For HT AlN optimization study, the AlN NL growth conditions are the same as for sample E. After the optimization of HT AlN growth, a 1.0-μm-thick HT AlN layer is grown with the molar V/III ratio of 483 and the growth temperature of 1,215°C for the HT AlN epilayers. The surface quality of the HT AlN layer, assessed by AFM, is shown in Fig. 5. A very clear and continuously linear step-flow pattern is observed on a 5 μm × 5 μm size image, which indicates very high crystalline quality.[5,6] On the 2 μm × 2 μm size image, shown in Fig. 5b, the equidistant terraces display saw-tooth shaped edges, which is very similar to what we have observed on AlN epilayers grown on AlN bulk substrates. Thus, such step-flow patterns with saw-tooth shaped terrace edges show that the epitaxial layer is of very high crystalline quality. The RMS roughness of Fig. 5a and b is 0.188 nm and 0.181 nm, respectively.

Figure 6 shows the (002) and (004) x-ray rocking curves obtained with triple-axis optics. The FWHMs of the (002) and (004) peaks are 11.5 arcsec and 14.5 arcsec, respectively. Our FWHM values are comparable to that of the best AlN *bulk* materials, which is about 10 arcsec for (002) peak, also measured by triple-axis optics.[11] The FWHMs of the (002) and (004) peaks measured by double-crystal optics are 32.4 arcsec and 54.4 arcsec, respectively. Both the triple-axis and double-crystal results are narrower than the values reported in the literature.[2,3] The FWHM of 155 arcsec is obtained in the asymmetric (104) peak rocking-curve scan measured by using double-crystal optics. The rocking curve (ω scan) of the (101) reflection is also measured by using double-crystal optics. The FWHM of 6804 arcsec for the (101) reflection is obtained, which indicates that the edge dislocation density is 3.2×10^{11} cm^{-2} using the evaluation procedure published in the literature.[12]

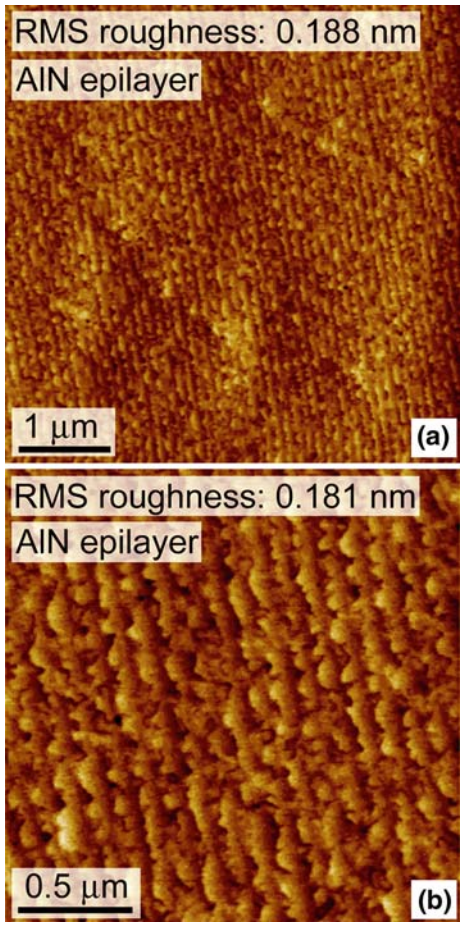

Fig. 5. AFM images of HT AlN surface grown on (0001) sapphire. (a) 5 μm × 5 μm image (b) 2 μm × 2 μm images.

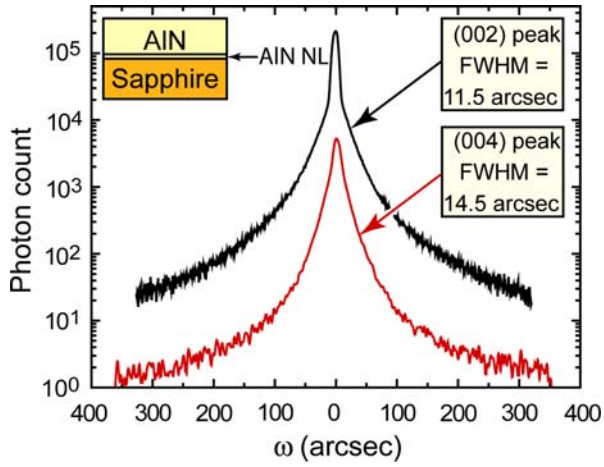

Fig. 6. X-ray rocking curves of HT AlN epilayer (002) and (004) peaks measured by triple-axis optics. A FWHM of 11.5 and 14.5 arcsec is obtained for the (002) and (004) reflection, respectively.

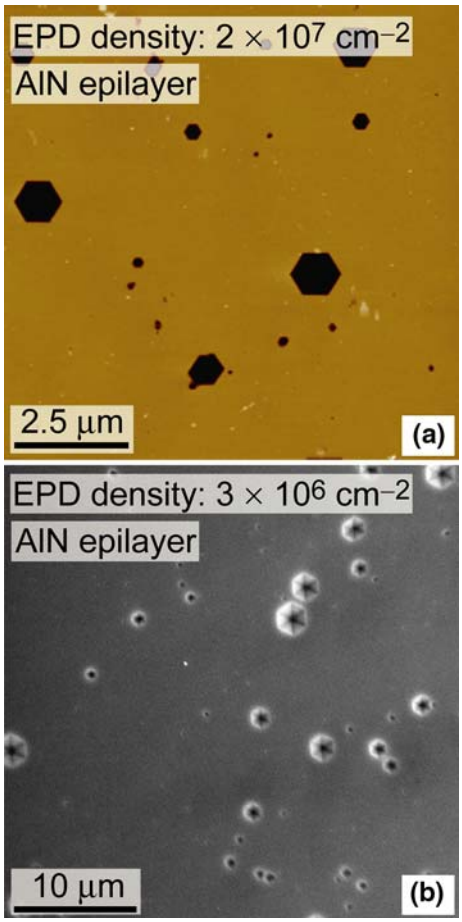

Fig. 7. (a) AFM image and (b) SEM image of KOH-etched AlN epilayer used to evaluate the etch-pit density.

In order to assess the surface quality, an EPD study is performed. The AlN sample is etched for 45 min in a 50% KOH solution heated to 70°C. The etched surface is measured by AFM and SEM, and the results are shown in Fig. 7. Before the SEM measurement, an 8-nm-thick Au film is *e*-beam deposited to work as a conductive layer. An EPD of 2×10^7 cm^{-2} is obtained from the AFM measurement, as shown in Fig. 7a, and 3×10^6 cm^{-2} from the SEM measurement, as shown in Fig. 7b, which is less than the AlN epilayers grown on SiC.[13] The EPDs measured by AFM are higher because the spatial resolution of AFM is better and sub-micron-scale etch pits can be observed more easily. By comparing the AFM and SEM results, we find that some very small etch pits are not detectable by SEM. Hence, AFM is the better technology to evaluate EPD density. To the best of our knowledge, the AlN presented here is the highest quality epilayer grown on sapphire reported to date.[14]

In conclusion, an optimization study of high-quality AlN epilayers grown on sapphire (0001) by metal-organic vapor-phase epitaxy is presented. It is found that for the nucleation optimization, TMAl flow is a most critical parameter, which determines the crystalline quality and surface morphology. An Al adatom diffusion enhancement model is presented to explain the strong dependence of the AlN epilayer crystalline and surface quality on the TMAl flow of the AlN NL. After the optimization, a very clear and continuously linear step-flow pattern is observed on AlN measured by AFM. A saw-tooth-shaped terrace edge of the step flow pattern indicates very high quality. The FWHMs of XRD rocking-curve scans are as narrow as 11.5 arcsec and thus even comparable with that of the best AlN bulk material. An EPD of 2×10^7 cm^{-2} is measured by AFM on KOH-etched AlN surfaces.

ACKNOWLEDGEMENTS

Support through Crystal IS, Department of Energy, ARO, the Samsung Advanced Institute of Technology, Sandia National Laboratories, NSF, and New York State is gratefully acknowledged. The authors acknowledge useful discussions with Dr. Thomas Gessmann and Mr. Jan-Yves Clames from Aixtron Inc.

REFERENCES

1. A.A. Allerman, M.H. Crawford, A.J. Fischer, K.H.A. Bogart, S.R. Lee, D.M. Follstaedt, P.P. Provencio, and D.D. Koleske, *J. Cryst. Growth* 272, 227 (2004).
2. J.P. Zhang, M.A. Khan, W.H. Sun, H.M. Wang, C.Q. Chen, Q. Fareed, E. Kuokstis, and J.W. Yang, *Appl. Phys. Lett.* 81, 4392 (2002).
3. X.Q. Shen, Y. Tanizu, T. Ide, and H. Okumura, *Phys. Status Solidi* C 0, 2511 (2003).
4. T.M. Katona, T. Margalith, C. Moe, M.C. Schmidt, S. Nakamur, J.S. Speck, and S.P. DenBaars, *Proc. SPIE* 5187, 250 (2004).
5. D.S. Green, S.R. Gibb, B. Hosse, R. Vetury, D.E. Grider, and J.A. Smart, *J. Cryst. Growth* 272, 285 (2004).
6. J.F. Kaeding, Y. Wu, T. Fujii, R. Sharma, P.T. Fini, J.S. Speck, and S. Nakamura, *J. Cryst. Growth* 272, 257 (2004).
7. K.B. Nam, J. Li, M.L. Nakarmi, J.Y. Lin, and H.X. Jian, *Proc. SPIE* 4992, 202 (2003).
8. F. Yan, M. Tsukihara, A. Nakamura, T. Yadani, T. Fukumoto, Y. Naoi, and S. Sakai, *Jpn. J. Appl. Phys.* 43, L1057 (2004).
9. R. Gaska, C. Chen, J. Yang, E. Kuokstis, M.A. Khan, G. Tamulaitis, I. Yilmaz, M.S. Shur, J.C. Rojo, and L. Schowalter, *Appl. Phys. Lett.* 81, 4658 (2002).
10. H. Amano, N. Sawaki, I. Akasaki, and Y. Toyoda, *Appl. Phys. Lett.* 48, 353 (1986).
11. B. Raghothamachar, M. Dudley, J.C. Rojo, Morgan, and L.J. Schowalter, *J. Cryst. Growth* 250, 244 (2003).
12. S.R. Lee, A.M. West, A.A. Allerman, K.E. Waldrip, D.M. Follstaedt, P.P. Provencio, and D.D. Koleske, *Appl. Phys. Lett.* 86, 241904 (2005).
13. D. Zhuang, J.H. Edgar, B. Strojek, J. Chaudhuri, and Z. Rek, *J. Cryst. Growth* 262, 89 (2004).
14. Y.A. Xi, K.X. Chen, F. Mont, X. Li, J.K. Kim, E.F. Schubert, C. Wetzel, W. Liu, and J.A. Smart, *Appl. Phys. Lett.* 89, 103106 (2006).